

## RESEARCH ARTICLE

# Concomitant sorting of circulating tumor cell subpopulations in cancer patients' blood samples through the multiplexed-immunosensor combination design

Phuong Lan Tran<sup>(1)\*</sup>, Yohann Tendero<sup>(2)</sup>, François Goldwasser<sup>(3)</sup>, Stanislas Ropert<sup>(3)</sup> and Romain Coriat<sup>(3)</sup>

**Authors' affiliations:**

- (1) FISHingCELL, 75014 Paris, France;
- (2) LTCI, Telecom ParisTech, Paris-Saclay University, 75013 Paris, France;
- (3) Department of Medical Oncology, Cochin-Broca-Hotel Dieu Teaching Hospital, Paris Descartes University, 75014 Paris, France.

\* **Corresponding author:** PL Tran, PhDs, e-mail: [phltran@orange.fr](mailto:phltran@orange.fr)

**Abstract**

Tumor cells that circulate in blood can initiate tumor metastases in distant sites. Circulating tumor cells (CTCs) are rare and heterogeneous, and display various phenotypes. The molecular characterization of each subpopulation is fundamental to its phenotypic identification and description of relevant genetic alterations for the management of patient's disease. We have previously described the development of a new mesofluidic multiplexed-immunosensor device for the capture and analysis of CTCs from blood samples of breast cancer patients. To aid sorting cancer cell subtypes for their characterization, we improve our methodology by serially interconnecting three-designed multiplexed-immunosensor devices that allowed grafting a subset of selective and specific antibodies for the capture of each cancer cell subtype. This new method gives a powerful tool to identify circulating tumor cell subtypes.

**Keywords:** Immunosensor, Mesofluidic, Multiplex device, Long alkylsilane monolayer, Targeted cell subpopulations capture, Circulating tumor cells (CTCs), Circulating endothelial cells (CECs)

**1. Introduction**

Tumor metastasis is the major cause of morbidity and death for cancer patients. A single tumor can include subclones with several phenotypes relevant to the development of metastatic disease (1). Circulat-

ing Tumor Cells (CTCs) that shed from primary tumors and metastases have become a helpful tool as liquid biopsy marker in cancer diagnostic (2). Evaluation of CTC subpopulations in cancer patients has a potential clinical value for correlation in disease staging or response to therapy (3,4).

CTCs may comprise heterogeneous subpopulations, epithelial and non-epithelial cells: circulating endothelial cells (CECs), cancer stem cells (CSCs), and those that have undergone the epithelial to mesenchymal transition (EMT) (5). Isolation of CTCs remains challenging. Most antibody-based methods used a unique anti-human EpCAM (epithelial cellular adhesion molecule) antibody for capture of epithelial CTCs (6-11). In the FDA-cleared CellSearch method, immunomagnetic coated-beads with anti-EpCAM antibody identified epithelial CTCs by cytokeratin-positivity, DAPI nuclear staining and CD45 negativity. We have developed a new immunosensor for selective capture of breast cancer cells, under laminar flow, onto antibody-coated long alkylsilane self-assembled monolayers in a parallel plate flow chamber (12-14). We then devised an mm-scale, mesofluidic multiplexed-immunosensor device embodying four parallel plate laminar flow chambers to prevent non-stable rheological phenomena in microfluidics (15,16). Its efficient analytic performance was demonstrated by the immobilization onto anti-EpCAM-coated AHTS (21-aminohenicosyl trichlorosilane) surfaces of CTCs from blood samples of metastatic and localized breast cancer patients (16). Microscopy data showed clear staining patterns of epithelial CTCs, positive for pan-cytokeratin antibodies and negative for leukocyte markers (CD45).

We now report a considerable improvement of heterogeneous CTC subpopulations sorting by a new design serially interconnecting three specified multiplexed-immunosensor devices that allowed grafting a subset of selective and specific antibodies for the capture of each cancer cell subtype. The performance of this specification was

demonstrated, from single patient blood sample, by concomitant capture of CTCs and CECs, which are among the representative biomarkers of liquid biopsies. This multiple detection was achieved for a low number of metastatic carcinoma: metastatic colorectal, metastatic prostatic, metastatic pancreatic, and metastatic kidney cancer. Blood samples from healthy individuals were analyzed in parallel and used as controls. CTCs were scored as pan-cytokeratin positive and CECs as VE-cadherin positive. Cell numbers were manually scored across laser scanning microscopy images of the full device. Cell numbers were highly consistent across duplicate chambers. This study was successful in addressing a technical challenge.

## **2 Materials and methods**

### **2.1. Glass surface silanization and antibody coupling**

Glass substrate and silane film preparation were performed as previously described (13,17). Standard microscopy glass slides were silanized under Ar atmosphere with *N*-protected AHTS [*N*-(21-trichlorosilanyl)henicosyl]-phthalimide], and deprotection of the amino group of AHTS (21-aminohenicosyl trichlorosilane), performed as described (13,17,18).

A non-exhaustive list of markers, which may be used to target the epithelial CTCs and the non-epithelial CTCs, is displayed in Tables 1 and 2, as well as the suppliers for purified monoclonal or polyclonal antibodies for cell capture and cell identification. An anti-CD45 antibody identified leukocytes. Molecular Probes (ThermoFisher Scientific, France) supplied all conjugated fluorescent secondary antibodies.

**Table 1.** Antibodies for epithelial subpopulation capture.

<i>Cell type</i>	<i>Markers</i>	<i>Antibody for epithelial subpopulation isolation (Suppliers)</i>
Epithelial	EpCAM, MUC 1	Monoclonal anti-human EpCAM; Monoclonal anti-human MUC 1 (R&D Systems, Lille, France)
Epithelial	Pan –cytokeratin	Polyclonal or monoclonal anti- Pan–cytokeratin (Abcam, Cambridge UK)

**Table 2.** Antibodies for non-epithelial subpopulation capture.

<i>Cell type</i>	<i>Markers</i>	<i>Antibody for non-epithelial subpopulation isolation (Suppliers)</i>
Endothelial	MCAM, VE-Cadherin	Monoclonal anti-MCAM, and anti-VE-Cadherin (R&D Systems, Lille, France)
Mesenchymal	N-cadherin, Cadherin 11, Vimentin, CSV Vimentin	Monoclonal anti-N-cadherin, anti-Cadherin 11, anti-Vimentin (Abcam, Cambridge UK) Monoclonal anti- CSV Vimentin (Abnova, Taiwan)
Leukocyte	CD45	Monoclonal anti-CD45 (Abcam, Cambridge UK)

Antibody immobilization on the silane-coated glass surface for capture was performed with either the monoclonal anti-EpCAM, or anti-MCAM (melanoma cell adhesion molecule), or anti-N Cadherin, or anti-CD45 antibodies in MES-buffered saline (2-[morpholino]-ethanesulfonic acid), 0.09% NaCl, pH 4.7 (Perbio Science, Brebières, France) at a concentration of 1mg/mL in the presence of 1-ethyl-3-(3-dimethylaminopropyl) carbodiimide hydrochloride (EDC, Perbio Science, France) overnight at 4°C. All slides were then washed in PBS and stored at 4°C under Ar atmosphere up to two weeks until use. In negative controls, AHTS-coated surfaces were grafted with specific species' isotypes IgG (Abcam, Cambridge UK). Quality controls were performed as described (13).

## **2.2. Embodiment of serially interconnected multiplex devices comprising four parallel plate laminar flow chambers and multi-option for antibody coating**

The physical characteristics of the mesofluidic multiplex device embodying four parallel plate laminar flow chambers whose each chamber is of dimensions 6x16x0.5 mm (WxLxH) were previously reported (15-16). The progressive laminar flow in the four laminar flow chambers was described (16). Each multiplex device is a proprietary product incorporated in a CapCelTec® package. They are manufactured by injection of cyclic olefin copolymer by a plastics industrialist.

Sorting target cells in a blood sample was optimized as follows: three multiplex devices, comprising a device with a tank and

2 devices tankless, were serially interconnected (19), as illustrated in Figure 1. The circulating flow was supplied by a tank through a single channel to the entrance of the four laminar flow chambers of the first row (device 1). The outlet of each chamber of device 1 was connected to the inlet of each chamber of the second row (device 2). Then the outlet of each chamber of device 2

was connected to the inlet of each chamber of the third row (device 3). Lastly, for the current configuration including three devices, the outlet of each chamber of device 3 was connected to a four-channels peristaltic pump (Watson Marlow, VWR, France), as shown in Figure 2. Laminar flow rate ranged from 400 to 600  $\mu\text{L}/\text{min}$ .

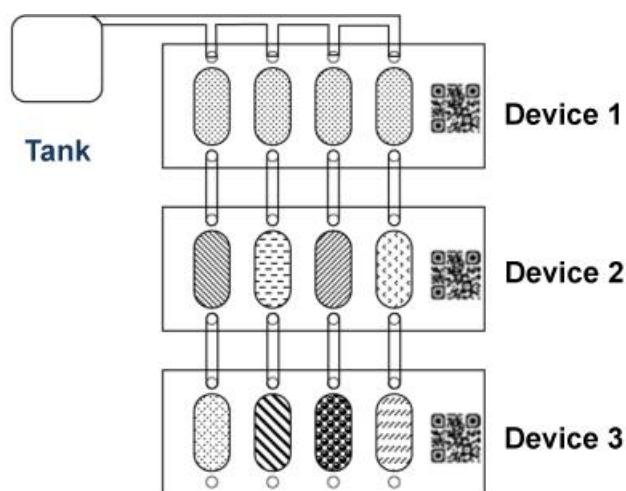


**Figure 1.** Serial combination of three multiplex devices CapCelTec®, comprising a device with a tank and 2 tankless devices. The first row includes an inlet fluidically connected to a tank (device 1). All devices are serially interconnected (device 1 to 3).



**Figure 2.** Connection of three multiplexed-immunosensor devices, CapCelTec®, comprising a device with a tank and 2 tankless devices, to a 4-channels peristaltic pump.

### 2.3. Patient Samples

Patients selected for this study were diagnosed with a metastatic colorectal adenocarcinoma, a metastatic prostatic, a metastatic pancreatic, or a metastatic kidney carcinoma (Cochin Hospital, Paris, France). The patient record was reviewed only to confirm the disease status, and no information on treatments or clinical course was abstracted.

Patients gave verbal consent to donate 8 mL of blood for this research study. All blood samples were drawn into heparin plus EDTA (ethyl-diamine-tetraacetic acid) Vacutainer tubes (Becton Dickinson, Pont de Claix, France). They were diluted into RPMI (Roswell Park Memorial Institute, USA) medium containing 10% fetal calf serum (FCS), 2mM glutamine, 100U/mL penicillin, and 100 $\mu$ g/mL streptomycin (Gibco, Thermofisher, France), and submitted to a Ficoll-Hypaque density-gradient centrifugation at 1600xg for 15 min at 15°C. The entire volume of the compartment with interphase nucleated-leukocyte cells was poured into a fresh centrifugation tube. Cells were centrifuged with washing buffer at 200xg for 10 min at 4°C. They were then used immediately, or frozen in complete RPMI medium containing 10% DMSO (dimethylsulfoxide) in liquid N<sub>2</sub> for subsequent cell capture experiments. Control blood samples from healthy volunteers were processed as above.

### 2.4. Cell isolation in multiplex parallel plate laminar flow chambers

Optimized sorting of target cells used one device for negative selection and two de-

vices for positive selection of CTC subpopulations. Antibody coating in each AHTS-coated glass surface remained very flexible. This is the quintessence of the methodology since the functionalized standard microscope glass slide allows a custom grafting of one or multiple antibodies targeting the capture of one or more CTC subpopulations.

The depletion of leukocytes by an anti-CD45 antibody grafted in the first row of all four AHTS-coated glass surfaces allowed performing a negative selection (device 1, Table 3 and Figure 3). Then multiple optional choices to functionalize each AHTS-coated glass surface by a specific and selective antibody for positive selection of CTC subpopulations could be subsequently applied to devices 2 and 3. As such for our present experiments (Table 3 and Figure 3), in device 2, two AHTS-coated glass surfaces were grafted with the monoclonal anti-human EpCAM antibody for capture of epithelial CTCs, and two AHTS-coated glass surfaces with the monoclonal anti-human anti-MCAM antibody for capture of CECs. In device 3, the order of grafting monoclonal anti-human EpCAM antibody and monoclonal anti-human anti-MCAM antibody could be inverted, as schematized in Table 3 and Figure 3. For devices 2 and 3, another couple of monoclonal antibodies could also be used such as the monoclonal anti-human EpCAM antibody for capture of epithelial CTCs and the monoclonal anti-human N Cadherin antibody for capture of mesenchymal CTCs. Negative controls were performed with cells loaded onto two AHTS-coated glass surfaces alone and two AHTS-coated glass surfaces grafted with specific species' isotypes IgG.

**Table 3.** Various antibodies grafting in serially interconnected three multiplex devices containing four laminar flow chambers. In each device, specific antibody grafting was selected for each laminar flow chamber #1 to #4.

Various antibodies grafting in serially connected three multiplex devices containing four laminar flow chambers				
	Chamber #1	Chamber #2	Chamber #3	Chamber #4
Device 1	Anti-CD45 antibody	Anti-CD45 antibody	Anti-CD45 antibody	Anti-CD45 antibody
Device 2	Anti-EpCAM antibody	Anti-EpCAM antibody	Anti-MCAM antibody	Anti-MCAM antibody
Device 3	Anti-MCAM antibody	Anti-MCAM antibody	Anti-EpCAM antibody	Anti-EpCAM antibody

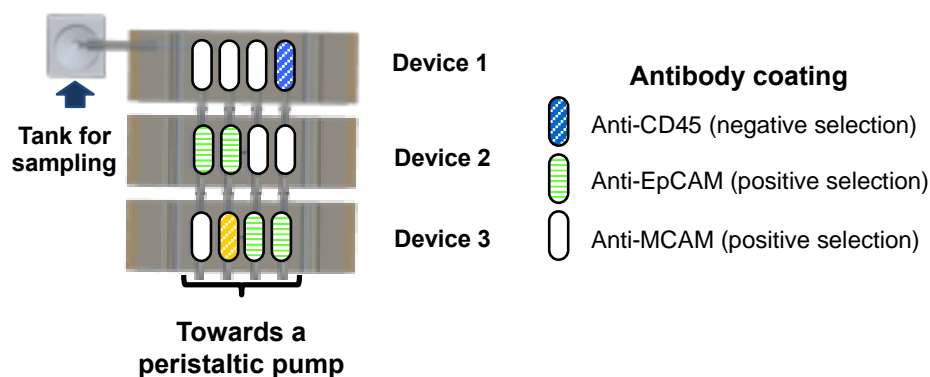


**Figure 3.** Outlines of one of the multiple options of grafting antibodies onto the AHTS-coated glass slide surfaces. Device 1 including 4-grafted AHTS glass slide surfaces was coated with monoclonal anti-CD45 antibody for depletion of leukocytes (chambers 1 to 4). Positive selection of epithelial CTCs and CECs subpopulations in device 2 was processed as follows: 2 grafted AHTS-coated glass slide surfaces with monoclonal anti-EpCAM antibody (chambers 1 and 2) and 2-grafted AHTS-coated glass slide surfaces with monoclonal anti-MCAM antibody (chambers 3 and 4); for device 3, the order of antibody grafting monoclonal was inverted: 2-grafted AHTS-coated glass slide surfaces with monoclonal anti-MCAM antibody (chambers 1 and 2), and 2 grafted AHTS-coated glass slide surfaces with monoclonal anti-EpCAM antibody (chambers 3 and 4).

Cell captures were performed with four milliliters of isolated nucleated-leukocyte cells, suspended in HBSS plus 0.3% human serum albumin (HSA, Sigma-Aldrich) to a dilution of  $10 \times 10^6$  cells/mL as reported (13,16). They were loaded in the tank and a flow rate of 400  $\mu\text{L}/\text{min}$  was applied to the entrance of the channel of distribution for driving cells into the flow chambers, until all entire active surfaces of the three devices were covered. Then 12-min cell incubation was performed at room temperature under stable conditions. At the end of the

incubation period, non-specifically bound cells were flushed with PBS at a flow rate of 600  $\mu\text{L}/\text{min}$  for 6 min.

### 2.5. Immunofluorescence staining and identification of CTC subpopulations by fluorescence microscopy

Fixation of cells was performed with 3mL cold acetone *in situ* in the devices for 5 min. Cell labeling was processed with subsequent various cell markers, as previously reported (13). Briefly, epithelial CTCs were

labeled by the primary polyclonal anti-pan cytokeratin antibody, CECs labeled by the primary monoclonal anti-VE Cadherin antibody and leukocytes by anti-CD45-APC antibody (Dako, Agilent, USA), then followed by secondary anti-rabbit Alexa-conjugated IgG and anti-mouse Alexa-conjugated IgG antibodies (Molecular Probes – ThermoFisher Scientific, France), respectively, according to Tran et al. (20). Cell nuclei were labeled with DAPI (1 µg/mL) for 5 min.

All slides were analyzed on an inverted NIKON E50i (NIKON, France) microscope equipped with an automated stage (IMSTAR, France). Four capture surfaces of each slide were scanned automatically in a 1360x1024 pixels format using the programmable stage and capture software (version 6, imaging IMSTAR systems, France). Captured images at 10X magnification were carefully examined with cells that stained positive by the primary rabbit polyclonal anti-pan-cytokeratin antibody and secondary Alexa-conjugated anti-rabbit IgG (green fluorescence). Their phenotypic morphological characteristics were taken into account as criteria for their selection and scored as epithelial CTCs, as described in Breton et al (16). Cells that stained positive by the mouse monoclonal anti-VE Cadherin antibody and secondary Alexa-conjugated anti-mouse IgG (red fluorescence) were scored as CECs. The same cells were stained by DAPI (blue stain) and negatively stained by anti-CD45-APC. As a remark, only a mouse monoclonal anti-VE Cadherin antibody was commercially supplied. No production of the monoclonal anti-VE Cadherin or the monoclonal anti-human MCAM antibodies in another animal host could be identified. Due to the coating of mouse monoclonal anti-human MCAM for capturing CECs subpopulation, staining with secondary

Alexa-conjugated anti-mouse IgG could result in a red fluorescence background, which did not have any impact for the CEC identification.

## **2.6. Hybridization of epithelial CTC subpopulations and fluorescence microscope**

All glass slides containing epithelial and non-epithelial CTCs, immobilized in the four functionalized surfaces imprinted on the glass slide, were treated in 100mM glycine in PBS-0.1 % Tween, pH2.7 for 2 min, then neutralized in Tris-HCl 0.5M, pH7.5. The slides were rinsed in PBS-0.1 % Tween and PBS. This process allowed eliminating cellular fluorescence and preserved the integrity of nuclei. They were then dehydrated in ethanol (70:85:100%). Interphase fluorescent *in situ* hybridization (FISH) was then performed. Pretreatment and denaturation of slides are carried out, as described in details by Fehm et al. (21). Kreatech (Leica Biosystems, Germany) provided Poseidon™ TMRSS2-ERG and Poseidon™ PTEN for chromosome analysis in prostatic cancer, and Poseidon™ EGFR for chromosome analysis in colorectal cancer.

FISH analysis was performed on 90i microscope equipped with a 63X objective (NA of 0.63) and filter cubes that permitted the acquisition of the fluorescence signals from DAPI and PlatinumBright-415, -495, -550 (Nikon Instruments Europe, France).

## **3 Results**

### **3.1. Capture of Circulating Tumor Cell subpopulations from cancer patients' blood**

We have developed a mesofluidic multiplexed-immunosensor device embodying four parallel plate laminar flow chambers

printed on a standard microscope glass slide functionalized with long amino-silane AHTS chains (16). This multiplexed-immunosensor device skillfully demonstrated the advantage to increase the number of capture surfaces for CTCs in once, and offered numerous opening possibilities for antibody grafting and helping to discriminate each CTC subpopulation. One to four different antibodies can be grafted on the four AHTS-coated surfaces of each mesofluidic multiplex device (16).

Taking advantage of this innovation, we optimize here the capture of CTC subpopulations by designing a new process interconnecting serially at least three mesofluidic multiplexed-immunosensor devices by manufacturing two types of devices, one with a tank and one tankless. Therefore, this design allows introducing in the same process a negative selection as the depletion of leukocytes by grafting AHTS-coating glass slide of device 1 with a monoclonal anti-CD45 antibody. The two other devices 2 and 3 were destined to the positive selection of CTC subpopulations (Figure 3). As described in section 2.4, the monoclonal anti-EpCAM antibody was grafted along with the monoclonal anti-MCAM antibody, each antibody separately in duplicate onto AHTS-coated surfaces (device 2). The monoclonal anti-EpCAM and monoclonal anti-MCAM antibodies are essential in targeting both CTC and CEC subpopulations, respectively. Unlike the order of antibody grafting in device 2, that of antibody grafting in device 3 is reversed. As shown in previous studies, the order of antibodies grafting on each of the four surfaces for capturing cells expressing various surface antigens should not have any impact on cell immobilization efficiency (16).

Having validated the multiplexed-immuno-

sensor with control breast cancer-derived cells and with blood samples from breast cancer patients, we evaluated now the capacity of the present novel design to concomitant capture CTC and CEC subpopulations from cancer patients' blood samples of other epithelial malignancies. Patients' blood samples included metastatic colorectal (n=5), metastatic prostatic (n=3), metastatic pancreatic (n=1), and metastatic kidney (n=1) carcinomas. Blood samples from two healthy donors were also provided. Identification of immobilized CTCs and CECs on each surface capture of both mesofluidic multiplex devices 2 and 3 consisted of staining with 4,6-diamino-2-phenylindole (DAPI) for DNA content, anti-pan-cytokeratin antibodies for epithelial CTCs, anti-VE-cadherin for CECs, and anti-CD45 antibody for leukocytes. Captured cells staining positive for pan-cytokeratin and negative for leukocyte markers recorded as epithelial CTCs are shown in Figure 4: a CTC from a metastatic colorectal (a), a metastatic prostatic (c), a metastatic pancreatic (e), and a metastatic kidney (g) cancer patient, respectively. The morphological characteristics exhibited by the captured CTCs were consistent with malignant cells, including large cellular size with high nuclear:cytoplasmic ratio. Captured cells staining positive for VE-cadherin were recorded as CECs from a metastatic colorectal (b), a metastatic prostatic (d), a metastatic pancreatic (f), and a metastatic kidney (h) cancer patient. CECs display a membrane labeling with a punctuate pattern (22). Figure 4 also shows pictures (20X) of capture of CTC (A) and CEC (B), respectively, and leukocytes from a metastatic prostatic cancer. A normal endothelial cell is displayed in Figure 4-C. Cell viability of captured cells was assessed under transmission light using Trypan blue that attested integrity of the cell membrane.

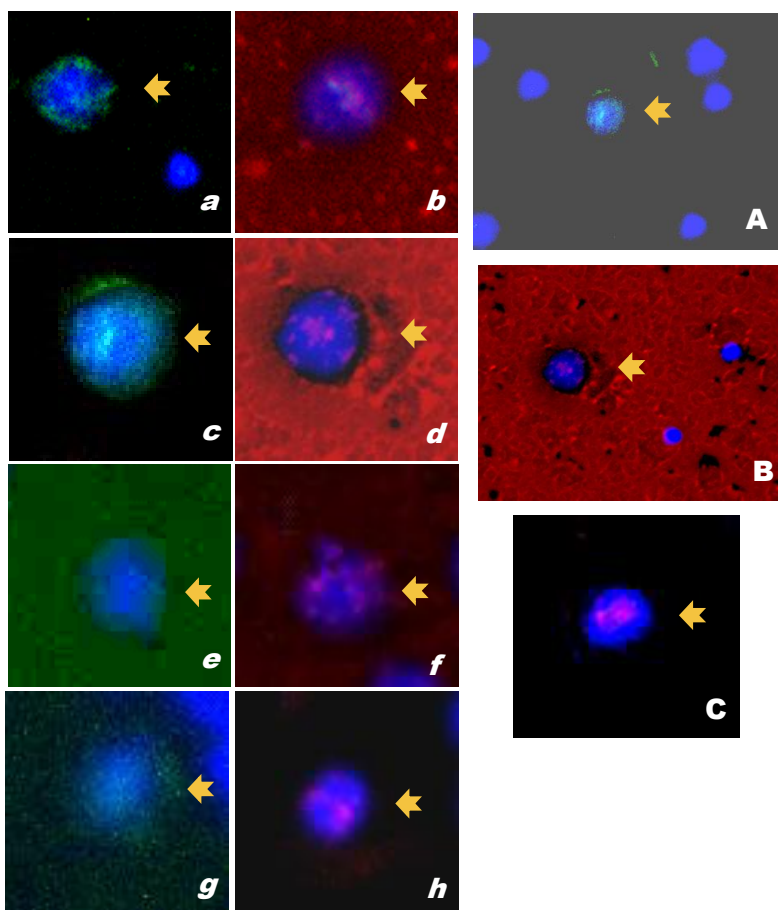


**Figure 4. Identification of CTCs and CECs from metastatic cancer patients.** Images of CTCs positively stained with an anti-pan-cytokeratin antibody and a secondary anti-rabbit A488-IgG and negatively with anti-CD45-APC antibody from metastatic colorectal (*a*), metastatic prostatic (*c*), metastatic pancreatic (*e*), and metastatic kidney (*g*) cancer patients. Images of CECs positively stained with an anti-VE Cadherin and a secondary anti-mouse A594-IgG from metastatic colorectal (*b*), metastatic prostatic (*d*), metastatic pancreatic (*f*), and metastatic kidney (*h*) cancer patients. Picture (20X) of a typical captured CTC and leucocytes from a metastatic prostatic cancer patient (A). Picture (20X) of a typical captured CEC and leucocytes from a metastatic prostatic cancer patient (B). Image of a normal endothelial cell stained with an anti-VE Cadherin and a secondary anti-mouse A594-IgG is displayed (C). Nuclei are stained with DAPI.

Table 4 displays the number of blood samples evaluated following concomitant captures of CTC and CEC subpopulations from patients with metastatic colorectal, metastatic prostate, metastatic pancreas, and metastatic kidney cancer, and from healthy donors. All blood samples were analyzed in duplicate. The number of CTCs ranged as follows: from 335 to 1035 per 3 mL ( $459 \pm 132$ , mean  $\pm$ S.D.) for colorectal cancer;

from 238 to 721 per 3 mL ( $482 \pm 176$ , mean  $\pm$ S.D.) for prostate cancer; from 112 to 371 per 3 mL ( $200 \pm 118$ , mean  $\pm$ S.D.) for pancreas cancer; from 112 to 371 per 3 mL ( $188 \pm 124$ , mean  $\pm$ S.D.) for kidney cancer. None of the 2 healthy donor blood samples had any identifiable CTC. The number of CECs ranged as follows: from 318 to 662 per 3 mL ( $532 \pm 185$ , mean  $\pm$ S.D.) for colorectal cancer; from 456 to 1315 per 3 mL

( $841 \pm 262$ , mean  $\pm$ S.D.) for prostate cancer; from 341 to 941 per 3 mL ( $618 \pm 282$ , mean  $\pm$ S.D.) for pancreas cancer; from 353 to 912 per 3 mL ( $559 \pm 244$ , mean  $\pm$ S.D.) for kidney cancer. Normal CECs ( $< 10$ cells/mL) could be identified in both healthy donor blood samples (range 9-32,

$21 \pm 9$ , mean  $\pm$  S.D.). As previously reported (13,16), concomitant capture of epithelial CTCs and CECs, respectively, yielded high performance of cell immobilization onto anti-EpCAM- and anti-MCAM-coated AHTS surfaces.

**Table 4.** Summary of CTC and CEC counts in 3 mL of blood from healthy donors and from metastatic colorectal, metastatic prostatic, metastatic pancreatic and metastatic kidney cancer patients. All blood samples were analyzed in duplicate. Cell counts are reported as mean  $\pm$  S.D.

Subjects	No of patients	No of analyzed samples	Range	Cell counts in 3 mL of blood Mean $\pm$ SD
Healthy No of CTCs No of CECs	2	4	0-0 9-32	$0 \pm 0$ $21 \pm 9$
<b>Colorectal cancer</b> No of CTCs No of CECs	5	10	335-1035 318-662	$459 \pm 132$ $532 \pm 185$
<b>Prostate cancer</b> No of CTCs No of CECs	3	6	238-721 456-1315	$482 \pm 176$ $841 \pm 262$
<b>Pancreas cancer</b> No of CTCs No of CECs	1	2	112-371 341-941	$200 \pm 118$ $618 \pm 282$
<b>Kidney cancer</b> No of CTCs No of CECs	1	2	112-371 353-912	$188 \pm 124$ $559 \pm 244$

### 3.2. Analysis of interphase nuclei by FISH

Following elimination of the fluorescent cellular pattern on each microscope slide containing four imprinted laminar flow chambers, the surfaces containing epithelial CTCs were labeled with FISH probes. Only the epithelial CTCs from metastatic colorectal and metastatic prostatic cancer patients were probed. In metastatic colorectal cancer, identification of molecular predictive factors is required in anti-EGFR therapies. Assessment of increased *EGFR* gene copy number by FISH could help identifying the chemotherapy refractory colorectal

patients most suitable for treatment with the anti-EGFR antibody (22, 23). Therefore, Figure 5A displays a result of *EGFR* gene amplification by FISH in a single CTC from a patient with metastatic colorectal cancer. Two genomic alterations in metastatic prostatic cancer were assayed by FISH: first, the alterations of the *ERG* locus when *TMPRSS2* gene fusions to the *ERG* gene. This early event is associated with invasion and can be addressed as a mechanism-based prognostic indicator (24,25). In one patient, we observed among several patterns a deletion of a *TMPRSS2-ERG* genes fusion and a break of *TMPRSS2*, as

shown in Figure 5B. Second, another genomic aberration that is detected in patients with metastatic prostatic cancer is the deletion of the *PTEN* gene. It is a common event associated with invasion with fre-

quencies 38-62% (26). Assessment of *PTEN* gene deletion in a single CTC from metastatic prostatic cancer is displayed in Figure 5C.

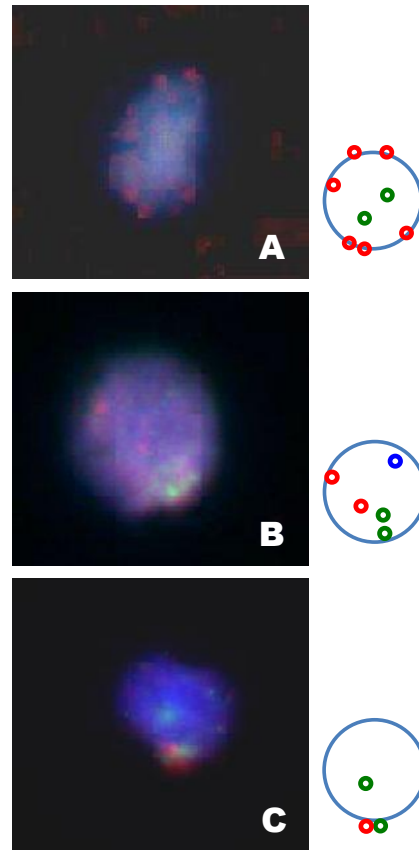


**Figure 5 A-C.** (A) FISH image of an epithelial CTC interphase nucleus from a metastatic colorectal cancer assessed by a dual-color *EGFR* assay for the detection of amplification at 7p11. Amplification involving the *EGFR* gene region at 7p11 shows 6 red signals, while the control at the chromosome 7-centromere region provides 2 green signals. (B) FISH image of a CTC interphase nucleus from a metastatic prostatic cancer assessed by a triple-color *TMPRSS2-ERG* assay for the detection of deletion of a *TMPRSS2-ERG* genes fusion and a break of *TMPRSS2*. Several patterns were found. FISH image that displays herein shows two red signals, one blue signal, and 2 green signals. (C) FISH image of an epithelial CTC interphase nucleus from a metastatic prostatic cancer assessed by a dual-color *PTEN* assay for the detection of deletion at 10q23. Deletion involving the *PTEN* gene region at 10q23 shows one red signal, while the control at the chromosome 10-centromere region provides 2 green signals.

#### **4 . Discussion**

Our technology approach is based on cell attachment under flow, which requires

high-affinity and high specificity binding of cell antigens to antibodies. We applied this process to our mesofluidic multiplexed-immunosensor. To amplify the number of

CTCs capture, we serially interconnected three mesofluidic multiplexed-immunosensors that allowed increasing the number of surface captures for their immobilization. New performances for high cell detection sensitivity are reported for the combination design embodying serially three-mesofluidic multiplexed-immunosensors in concomitant capture of heterogeneous subpopulations of CTCs. The serial system benefits from the already demonstrated characteristics of laminar flow chambers at mm-scale reducing the rheological phenomena of microfluidics. We demonstrate here its analytical capacity to concomitantly immobilize epithelial CTC and CEC subpopulations from various cancer patients' blood samples, namely metastatic colorectal, metastatic prostatic, metastatic pancreatic and metastatic kidney cancer, as reported in the results section. The primary tumor in most cases of patients with colorectal cancer can be easily controlled but distant metastases ultimately limit the patient's prognosis (27-29). Evaluation of CTCs could be regarded as a prognostic and/or predictive value (30). Same as for CRC cancer, analysis of CTCs from patients with metastatic castration-resistant prostatic cancer predicts benefit responses from treatment (31,32). In pancreatic cancer, a highly malignant tumor with poor prognosis (33), CTCs analysis may yield insight into the process of metastasis and provides prognostic and predictive information (34-37). Kidney cancer is not a single disease but comprises a number of different cancers that occur in the kidney, each with a different histology (38). Renal cell cancer (RCC) is the most frequent solid lesion of kidney (38). The correlation of detection of CTCs in peripheral blood of RCC patients with prognosis can have an impact on detection of early metastases and may serve as a marker for monitoring therapeutic efficacy

(39). Evaluation of CECs in cancer, a non-epithelial cell subpopulation, and seemingly a marker of vascular damage shed in peripheral blood (40), provides a prognostic indicator. Among characteristic endothelial cell markers, membrane MCAM and VE-cadherin are highly expressed in CECs (41). CECs are present in abnormally high numbers and might reflect the abnormal high turnover rate of tumor endothelium, as well as the disordered nature of tumor angiogenesis. The intensity of angiogenesis could predict the probability of invasive tumor and metastasis (42). CECs are sized from 20 to 50  $\mu\text{m}$ . The new mesofluidic multiplexed-immunosensors combination design enables high sensitivity and specificity for concomitant capture and purification of large number of viable epithelial CTC and CEC subpopulations. The multiplexed-immunosensor combinations offer a versatile tool readily grafted with a variety of purified antibodies onto AHTS-coated standard microscope slides, and is destined to optimizing concomitant capture of CTC subpopulations such as mesenchymal CTCs, cancer stem cells (CSC), in addition to epithelial CTCs and CECs demonstrated in the present study. Such active glass surface also provides not only an ideal transparent surface for fluorescence microscopy, but also a surface easily processed for cellular, genetic and genomic analyses. We demonstrated that the same slide containing immobilized-epithelial CTCs was readily assessed for genomic aberrations and alterations. FISH assays of liquid biopsy are regularly and easily accessed for controls than the paraffin-embedded tissue blocks. Lastly, this new combination design addresses a diagnostic tool for predictive and prognostic biomarkers of liquid biopsy that can be destined to all options for the clinical management of patients with cancer.

## ACKNOWLEDGEMENTS

Dr Bernard Bennetau is thanked for his expertise in surface chemistry, Dr Louis Renaud for his expertise in fluid mechanics, Dr Jérôme Darbon and Dr Marc Sigelle for expert advices, Dr Patric Tauc for his expertise in photonics, and François Breton for skillful assistance in mechanics engineering. Pr Jean-Claude Ehrhart is thanked for reading this manuscript. This work was supported in part by contracts from the Direction de la Politique Industrielle (CNRS #63875), OSEO (AIMA, #A 10 11 060 Q), and private funding.

## Bibliography

1. Yu M, Bardia A, Wittner BS, Stott SL et al. Circulating breast tumor cells exhibit dynamic changes in epithelial and mesenchymal composition. *Science* 2013; 339:580-584.
2. Brock G, Castellanos-Rizaldos E, Hu L et al. Liquid biopsy for cancer screening, patient stratification and monitoring. *Transl Cancer Res* 2015;4:280-290.
3. Cohen SJ, Punt C JA, Iannotti N, Saidman BH et al. Relationship of circulating tumor cells to tumor response, progression-free survival, and overall survival in patients with metastatic colorectal cancer. *J Clin Oncol* 2008; 19 3213-3221.
4. Alix-Panebières C, Pantel K. Challenges in circulating tumor cells research. *Nat Rev Cancer* 2014; 14:623-631.
5. Barriere G, Fici P, Gallerani G et al. Circulating tumor cells and epithelial, mesenchymal and stemness markers: characterization of cell subpopulations. *Ann Transl Med* 2014;2:109-117.
6. Allard WJ, Matera J, Craig Miller M, Repollet M et al. Tumor cells circulate in the peripheral blood of all major carcinomas but not in healthy subjects or patients with nonmalignant diseases. *Clin Cancer Res* 2004; 10 :6897-6904.
7. Cristofanilli M, Budd T, Ellis M, Stopeck A et al. Circulating tumor cells, Disease progression, and survival in metastatic breast cancer. *N Engl J Med* 2004; 351:781-791.
8. Riethgdorf S, Fritsche H, Müller V, Rau T et al. Detection of circulating tumor cells in peripheral blood patients with metastatic breast cancer: a validation study of the CellSearch system. *Clin Cancer Res* 2007; 13:920-928.
9. Nagrath S, Sequist LV, Maheswaran S, Bell DW et al. Isolation of rare circulating tumor cells in cancer patients by microchip technology. *Nature* 2007; 450:1235-1241.
10. Saucedo-Zeni N, Mewes S, Niestroj R, Gasiorowski L et al. A novel method for the *in vivo* isolation of circulating tumor cells from peripheral blood of cancer patients using a functionalized and structured medical wire. *Int J Oncol* 2012; 41:1241-1250.
11. Ozkumur E, Shah AM, Ciciliano JC, Emmink BL et al. Inertial focusing for tumor antigen-dependent and -independent sorting of rare circulating tumor cells. *Sci Transl Med* 2013; 5:179-199.
12. Tran PL, Bennetau B. Novel microfluidic system and method for capturing cells. CNRS, FR00/07722 (2004).
13. Ehrhart JC, Bennetau B, Renaud L, Madrange JP et al. A new immunosensor for breast cancer cell detection using antibody-coated long alkylsilane self-

assembled monolayers in a parallel plate flow chamber. *Biosens. Bioelectr.* 2008; 24, 467-474.

14. Breton F, Tran PL. Sensitive mesofluidic immunosensor for detection of circulating breast cancer cells onto antibody-coated long alkylsilane self-assembled monolayers. *Biosensors and Molecular Technologies for cancer diagnostics*. CRC Press 2012; 377-389.

15. Tran PL, Régnier G, Breton F. Microfluidic device and method for implementing same. CNRS, FR00/00333 (2009).

16. Breton F, Bennetau B, Lidereau R, Thomas L et al. A mesofluidic multiplex immunosensor for detection of circulating cytokeratin-positive cells in the blood of breast cancer patients. *Biomed Microdevices* 2011; 13:1-9.

17. Bennetau B., Bousbaa J., Choplin F. Organosilicon compounds, preparation method and uses thereof. CNRS, FR00/00695 (2000).

18. Martin P, Marsaudon S, Thomas L, Desbat B. et al. Liquid mechanical behaviour of mixed monolayers of amino and alkyl silanes by atomic force microscopy. *Langmuir* 2005; 21:6934-6943.

19. Tran PL. Method and device for selective, specific and simultaneously sorting target rare cells in a biological sample. WO2016075410-EP3218111.

20. Tran PL, Deugnier MA. Intracellular localization of 12-O-3-N-dansylamino TPA in C3H/10T1/2 mouse cell line. *Carcinogenesis* 1985;6:433-439.

21. Fehm T, Sagalowsky A, Clifford E et al. Cytogenetic evidence that circulating epithelial cells in patients with carcinoma are malignant. *Clin Cancer Res* 2002; 8:2073-2084.

22. Solovey A, Lin Y, Browne P et al. Circulating endothelial cells in sickle cell anemia. *New Engl J Med*;1997;337:1584-90.

23. Cappuzzo F, Finocchiaro G, Rossi E et al. EGFR FISH assay predicts for response to cetuximab in chemotherapy refractory colorectal cancer patients. *Ann Oncol* 2008;19:717-723.

24. Attard G, Clark J, Ambroisine L et al. Duplication of the fusion of *TMPRSS2* to *ERG* sequences identifies fatal human prostate cancer. *Oncogene* 2008;27:253-263.

25. Perner S, Mosquera JM, Demichelis F et al. *TMPRSS2-ERG* Fusion prostate cancer: an early molecular event associated with invasion. *Am J Pathol* 2007;31:882-888.

26. Yoshimoto M, Cutz JC, Nuin PAS et al. Interphase FISH analysis of *PTEN* in histologic sections shows genomic deletions in 68% of primary prostate cancer and 23% of high-grade prostatic intra-epithelial neoplasias. *Cancer Gen Cytog* 2006;169:128-137.

27. Sartore-Bianchi A, Fieuws S, Veronese S et al. Standardisation of EGFR FISH in colorectal cancer: results of an international interlaboratory reproducibility ring study. *J Clin Pathol* 2012;65:218-223.

28. Barbazan J, Alonso-Alconada L, Muínelo-Romay L et al. Molecular characterization of circulating tumor cells in human metastatic colorectal cancer. *Plos one* 2012;7:1-8.

29. Schölch S, Bork U, Rahbari NN, Garcia S et al. Circulating tumor cells of colorectal cancer. *Cancer Cell & Microenvironment* 2014;1:1-5.

30. Yaeger R, Chatila WK, Lipsyc MD et al. Clinical sequencing defines the genomic landscape of metastatic colorectal cancer. *Cancer Cell* 2018;33:121-126.
31. De Bono JS, Scher HI, Montgomery RB et al. Circulating tumor cells predict survival benefit from treatment in metastatic castration-resistant prostate cancer. *Clin Cancre Res* 2008; 14:6302-6309.
32. Hu B, Rochefort H, Goldkorn A. Circulating tumor cells in Prostate cancer. *Cancers* 2013; 5:1776-1690.
33. Li D, Xie K, WolffR, Abbruzese JL. Pancreatic cancer. *The Lancet* 2004;363:1049-1057.
34. Kurihara T, Itoi T, Sofuni A et al. Detection of circulating tumor cells in patients with pancreatic cancer : a preliminary result. *J Hepatobiliary Pancreat Surg* 2008;15:189-195.
35. De Albuquerque A, Kubisch I, Breier G et al. Multimarker gene analysis of circulating tumor cells in pancreatic cancer patients : A feasibility study. *Oncology* 2012;82:3-10.
36. Khoja L, Backen A, Sloane R et al. A pilot study to explore circulating tumour cells in pancreatic cancer as a novel biomarker. *British J Cancer* 2012 ;106 :508-516.
37. Han L, Chen W, Zhao Q. Pronostic value of circulating tumor cells in patients with pancreatic cancer: a meta-analysis. *Tumor Biol* 2013; DOI 10.1007/s13277-013-1327-5.
38. Semeniuk-Wojtas A, Stec R, Szczylik C. Are primary renal cell carcinoma and metastases of renal cell carcinoma the same cancer? *Urol Oncol* 2016;34:215-220.
39. Bluemke K, Bilkenroth U, Meye A et al. Detection of circulating tumor cells in peripheral blood of patients with renal carcinoma correlates with prognosis. *Cancer Epidemiol Biomarkers Prev.* 2009;18:2190-2196.
40. Blann AD, Woywodt A, Bertolini F et al. Circulating endothelial cells-Biomarker of vascular disease. *Thromb Haemost* 2005.93:228-35.
41. Khan SS, Solomon MA, McCoy Jr JP. Detection of circulating endothelial cells and endothelial progenitor cells by flow cytometry. *Cytometry Part B* 2005;64B:1-8.
42. Weidner N, Carroll PR, Flax J et al. Tumor angiogenesis correlates with metastasis in invasive prostate carcinoma. *Am J Pathol* 1993;143:401-10.